Int. J. Heat Mass Transfer. Vol. 21, pp. 1221–1228

0017-9310/78/0901-1221 $02.00/0

INSTABILITY OF FREE CONVECTION FLOW OVER A HORIZONTAL IMPERMEABLE SURFACE IN A POROUS MEDIUM

C. T. HSU
Department of Civil Engineering

PING CHENG*
Department of Petroleum Engineering

and

G. M. HOMSY
Department of Chemical Engineering, Stanford University, Stanford, CA 94305, U.S.A.

(*Received* 27 *July* 1977 *and in revised form* 23 *January* 1978)

Abstract—A linear stability analysis is made to determine the conditions marking the onset of longitudinal vortices in free convective flow in a porous medium adjacent to a horizontal heated surface with a prescribed wall temperature. The basic state is assumed to be the steady two-dimensional buoyancy-induced boundary-layer flow which is characterized by a non-linear temperature profile. The transverse velocity component of the basic flow as well as the streamwise dependence of the basic flow and temperature fields are taken into consideration when deriving the three-dimensional perturbation equations for the secondary flow. The resulting variable coefficient eigenvalue problem is solved numerically, and the amplitudes and phase angles of the disturbances, as well as the streamlines and isotherms of the secondary flow at the onset of instability are shown. The effect of wall temperature distribution on the critical Rayleigh number and its associated wave number are discussed.

NOMENCLATURE

- a, wave number;
- A, constant in wall temperature relation;
- C, superposition constant;
- f, dimensionless base state stream function;
- F, dimensionless disturbance stream function;
- k, wave number;
- K, Darcy permeability;
- m, exponent on wall temperature relation;
- p, pressure;
- Ra_x, local Rayleigh number;
- t, time;
- T, temperature;
- u, Darcys' velocity component in x direction;
- v, Darcys' velocity component in y direction;
- $\bar{v}$, Darcys' velocity vector;
- w, Darcys' velocity component in z direction;
- x, coordinate in downstream direction;
- y, coordinate normal to bounding surface;
- z, coordinate tangent to bounding surface.

Greek symbols

- α, effective thermal diffusivity;
- β, coefficient of thermal expansion;
- γ, volumetric heat capacity of the fluid to that of the saturated porous medium;
- μ, fluid viscosity;
- η, similarity variable;
- Θ, dimensionless temperature;
- Ψ, stream function;
- σ, growth constant;
- ρ, fluid density.

*On sabbatical leave from the Department of Mechanical Engineering, University of Hawaii, Honolulu, HI 96822, U.S.A.

I. INTRODUCTION

IT HAS been established that when a fluid layer is heated from below, the presence of the buoyancy force component normal to the surface gives rise to vortex instability under critical conditions. The appearance of longitudinal vortices (or rolls) have been observed by Chandra [1], as well as by Akiyama, Hwang and Cheng [2] for forced convection between differentially heated parallel plates, and by Sparrow and Hussar [3] as well as by Lloyd and Sparrow [4] for natural convection on inclined heated surfaces. Motivated by these experimental investigations, a number of linear stability analyses have recently been performed to study the conditions marking the onset of longitudinal vortices in both free [5–8] and forced [9–11] convection in a fluid layer heated from below.

The occurrence of streamwise oriented vortices in a porous medium between two parallel inclined plates heated from below has been observed by Bories and Combarnous [12] who also performed a stability analysis which shows that the onset of secondary flow in the form of longitudinal vortices occurs when $Ra\cos\phi \geqslant 4\pi^2$, where ϕ is the inclined angle of the plates with respect to the horizontal and Ra is the Rayleigh number based on the distance between the plates. In Bories and Combarnous' analysis, both the temperature and velocity profiles of the basic flow are

linear functions of distance normal to the plates and independent of streamwise direction.

It is the purpose of this paper to study the related problem of onset of vortex instability in free convection flow in a porous medium adjacent to a heated horizontal surface where the prescribed wall temperature is a power function of distance. The basic undisturbed state is assumed to be the steady buoyancy-induced boundary layer flow which is characterized by a non-linear temperature profile [13]. The full three-dimensional disturbance equations are simplified on the basis of the so-called "bottling effects", i.e. the disturbances at the onset of instability are contained within the boundary layer of the basic flow [6]. The resulting eigenvalue problem is solved numerically by the fourth-order Runge–Kutta method incorporated with Kaplan filtering [14, 15] to maintain the linear independence of the two eigenfunctions. The amplitudes and phase angles of the disturbances, as well as the streamlines and isotherms of the secondary flow at the onset of instability are shown. The effects of wall temperature distribution on the critical Rayleigh number and its associated wave number are discussed.

II. LINEAR STABILITY ANALYSIS

Consideration is given to the problem of free convection in a porous medium adjacent to an impermeable heated surface with the prescribed wall temperature of the form $T_w(x) = T_\infty + Ax^m$, where T_w and T_∞ are temperatures at the wall and at infinity; A and m are constants which are positive and real. The coordinates of the problem are depicted in Fig. 1 where x and z are the coordinates that lie on the horizontal plane and y is the vertical coordinate pointing outward toward the porous medium. If we assume that (1) the

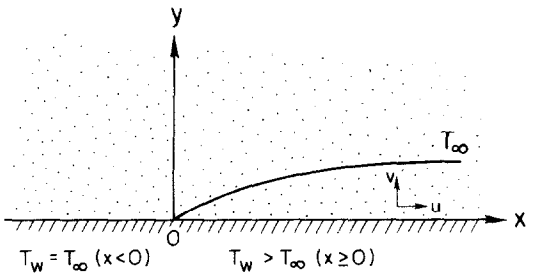

FIG. 1. Definition sketch.

convective fluid and the porous medium are everywhere in local thermodynamic equilibrium; (2) properties of the fluid and the porous medium, such as thermal conductivity, specific heats, viscosity, and permeability are constant; (3) the Boussinesq approximations are employed, and (4) Darcy's law is applicable, the governing equations for convective heat transfer in a porous medium are:

$$\nabla \cdot \bar{v} = 0, \tag{1}$$

$$\frac{\mu \bar{v}}{K} = -\nabla p' - \rho_\infty \beta g (T - T_\infty), \tag{2}$$

$$\gamma \frac{\partial T}{\partial t} + \bar{v} \cdot \bar{\nabla} T = \alpha \nabla^2 T, \tag{3}$$

where the subscript "∞" denotes the conditions at infinity.

A linear stability analysis will now be made by decomposing the temperature, velocity, and pressure distribution into basic undisturbed quantities and infinitesimal disturbed quantities as

$$\begin{aligned} T(x,y,z,t) &= T_0(x,y) + T_1(x,y,z,t), \\ p(x,y,z,t) &= p_0(x,y) + p_1(x,y,z,t), \\ u(x,y,z,t) &= u_0(x,y) + u_1(x,y,z,t), \\ v(x,y,z,t) &= v_0(x,y) + v_1(x,y,z,t), \\ w(x,y,z,t) &= w_1(x,y,z,t), \end{aligned} \tag{4}$$

where the three dimensional disturbances are denoted by the subscript "1" and the two dimensional basic quantities are denoted by the subscript "0". It will be assumed that the undisturbed basic state is that of steady two-dimensional buoyancy-induced boundary layer flow whose solution is given by Cheng and Chang [13] to be of the form

$$T_0(x,y) = T_\infty + Ax^m \theta_0(\eta), \tag{5}$$

and

$$\begin{aligned} \psi_0(x,y) &= \alpha (Ra_x)^{1/3} f_0(\eta), \\ \eta &= (Ra_x)^{1/3} y/x, \end{aligned} \tag{6}$$

where $Ra_x = K\rho_\infty g\beta(T_w - T_\infty)x/\mu\alpha$ is the Rayleigh number in a porous medium, and η is a similarity variable. As shown in [13], the dimensionless temperature $\theta_0(\eta)$ and stream function $f_0(\eta)$ are solutions of

$$f_0'' + m\theta_0 + \frac{m-2}{3}\eta\theta_0' = 0, \tag{7}$$

$$\theta_0'' - m\theta_0 f_0' + \frac{m+1}{3} f_0 \theta_0' = 0, \tag{8}$$

with boundary conditions given by

$$\theta_0(0) = 1, \quad f_0(0) = 0, \tag{9}$$

$$\theta_0(\infty) = 0, \quad f_0'(\infty) = 0, \tag{10}$$

where the primes on basic flow quantities indicate derivatives with respect to η.

Substituting equation (4) into equations (1)–(3), subtracting out the governing equations for the basic flow and linearing, we have

$$\frac{\partial u_1}{\partial x} + \frac{\partial v_1}{\partial y} + \frac{\partial w_1}{\partial z} = 0, \tag{11}$$

$$\frac{\mu u_1}{K} = -\frac{\partial p_1}{\partial x}, \tag{12}$$

$$\frac{\mu v_1}{K} = -\frac{\partial p_1}{\partial y} - \rho_\infty g\beta T_1, \tag{13}$$

$$\frac{\mu w_1}{K} = -\frac{\partial p_1}{\partial z}, \tag{14}$$

$$\gamma \frac{\partial T_1}{\partial t} + u_0 \frac{\partial T_1}{\partial x} + v_0 \frac{\partial T_1}{\partial y} + u_1 \frac{\partial T_0}{\partial x} + v_1 \frac{\partial T_0}{\partial y} = \alpha \left(\frac{\partial^2 T_1}{\partial x^2} + \frac{\partial^2 T_1}{\partial y^2} + \frac{\partial^2 T_1}{\partial z^2} \right). \tag{15}$$

where all terms arising from the transverse velocity component of the basic flow as well as the x-dependence of the basic flow and temperature fields have been retained.

From the related work of vortex instability in free convection about an inclined plate, it has been shown that small disturbances at the onset of instability are confined within the boundary layer of the basic flow because of the transverse inward-directed velocity component of the basic flow which entrains fluid on the plate. This has been termed the "bottling effect" by Haaland and Sparrow [6]. If the assumption of bottling effects are invoked, some of the terms in equations (11)–(15) can be neglected. This can be shown by first converting the equations in dimensionless form and then expressing the resulting equations in terms of the stretched boundary layer coordinates of the basic flow. We want to give the highlights of this argument, because it is subtle and does not seem to have been carefully detailed in the literature. The dimensionless forms of (11)–(15) are

$$\frac{\partial u_1}{\partial x}+\frac{\partial v_1}{\partial y}+\frac{\partial w_1}{\partial z}=0, \tag{16}$$

$$\frac{\partial p_1}{\partial x}=-u_1, \tag{17}$$

$$\frac{\partial p_1}{\partial y}=-v_1+RT_1, \tag{18}$$

$$\frac{\partial p_1}{\partial z}=-w_1, \tag{19}$$

$$\gamma\frac{\partial T_1}{\partial t}+v_0\frac{\partial T_1}{\partial y}+u_0\frac{\partial T_1}{\partial x}+v_1\frac{\partial T_0}{\partial y}+u_1\frac{\partial T_0}{\partial x}=\frac{\partial^2 T_1}{\partial x^2}+\frac{\partial^2 T_1}{\partial y^2}+\frac{\partial^2 T_1}{\partial z^2}, \tag{20}$$

where R is a Rayleigh number based upon a fictitious length which is of no consequence in the resulting similarity solution. For the base state, we have for large R [13], variations that are asymptotically

$$\frac{\partial}{\partial y}\sim R^{1/3}\frac{\partial}{\partial Y};\quad \frac{\partial}{\partial x}\sim 1;\quad v_0\sim R^{1/3};\quad u_0\sim R^{2/3}.$$

Now since $v_0<0$, any small disturbance will be convectively held ("bottled") on the plate, so that for vortex-like disturbances with wave length of the same scale as the base state thermal depth, we have for bottled disturbances,

$$\frac{\partial}{\partial y}\sim R^{1/3}\frac{\partial}{\partial Y};\quad \frac{\partial}{\partial z}\sim R^{1/3}\frac{\partial}{\partial Z};\quad \frac{\partial}{\partial x}\sim 1.$$

Equations (16)–(19) become

$$\frac{\partial v_1}{\partial Y}+\frac{\partial w_1}{\partial Z}+R^{-1/3}\frac{\partial u_1}{\partial x}=0, \tag{16a}$$

$$\frac{\partial P_1}{\partial x}=-u_1, \tag{17a}$$

$$R^{1/3}\frac{\partial P_1}{\partial Y}=-v_1+RT_1, \tag{18a}$$

$$R^{1/3}\frac{\partial P_1}{\partial Z}=-w_1. \tag{19a}$$

We wish to use (16a)–(19a) to estimate the relative orders of the convective terms in equation (20). Equation (16a) establishes that $v_1\sim w_1$ for a convective roll, and (19a) establishes $P_1\sim R^{-1/3}w_1$. Now a key point is that if there is an $O(1)$ x-variation in disturbance quantities, then equation (17a) implies $u_1\sim R^{-1/3}v_1$. There is necessarily this x-dependence through the variable coefficients in equation (20) involving the base state. Thus $P_1=P_1(x,Y,Z)$, and $u_1\neq 0$. The convective terms in equation (20) have the estimates

$$u_0\frac{\partial T_1}{\partial x}\sim R^{2/3}\frac{\partial T_1}{\partial x},$$

$$v_0\frac{\partial T_1}{\partial y}\sim R^{2/3}\frac{\partial T_1}{\partial Y},$$

$$u_1\frac{\partial T_0}{\partial x}\sim R^{-1/3}v_1\frac{\partial T_0}{\partial x},$$

$$v_1\frac{\partial T_0}{\partial y}\sim R^{1/3}v_1\frac{\partial T_0}{\partial Y}.$$

The first two terms are evidently of the same order. The next two estimates depend upon the ratio of v_1 to T_1, which is in fact related to the actual solution to the eigenvalue problem. We have retained all four terms in what follows. The important conclusion from (16a) and (17a)–(19a) is that

$$\frac{\partial v_1}{\partial y}+\frac{\partial w_1}{\partial z}=0 \tag{16b}$$

to lowest order, implying the existence of a disturbance stream function defined such that

$$v_1=-\frac{\partial\psi_1}{\partial z},\quad w_1=\frac{\partial\psi_1}{\partial y}. \tag{21}$$

We revert back to dimensional variables in order to properly develop the similarity solution. Equations (12)–(15) in terms of stream function are

$$\frac{\partial u_1}{\partial z}=\frac{\partial^2\psi_1}{\partial x\partial y}, \tag{22}$$

$$\frac{\mu}{K}\left(\frac{\partial^2\psi_1}{\partial y^2}+\frac{\partial^2\psi_1}{\partial z^2}\right)=-\rho_\infty\beta g\frac{\partial T_1}{\partial z}, \tag{23}$$

$$\gamma\frac{\partial T_1}{\partial t}+u_0\frac{\partial T_1}{\partial x}+v_0\frac{\partial T_1}{\partial y}+u_1\frac{\partial T_0}{\partial x}-\frac{\partial\psi_1}{\partial z}\frac{\partial T_0}{\partial y}=\alpha\left(\frac{\partial^2 T_1}{\partial y^2}+\frac{\partial^2 T_1}{\partial z^2}\right), \tag{24}$$

where

$$u_0=\left(\frac{\alpha}{x}\right)(Ra_x)^{2/3}f_0'(\eta)$$

and

$$v_0=-\left(\frac{\alpha}{x}\right)(Ra_x)^{1/3}\left[\frac{m-2}{3}\eta f_0'+\frac{m+1}{3}f_0\right].$$

It should be noted that the term $u_0(\partial T_1/\partial x)$ is retained in equation (24) since although $\partial T_1/\partial x$ is small, $u_0(\partial T_1/\partial x)$ is of the same order of magnitude as other convective terms in equation (24).

Hwang and Cheng [5] and Haaland and Sparrow [6] have neglected the term $u_0(\partial T_1/\partial x)$ in their analyses of onset of stability in a viscous fluid because all the disturbances are assumed to be independent of x. In fact the disturbance has a weak x dependence, which coupled with the strong convective base flow u_0, leads to retention of this term at lowest order.

Experimental evidence shows that small disturbances in the form of longitudinal vortices are periodic in the spanwise direction. Thus, we assume that the three-dimensional disturbances are of the form

$$\psi_1 = \hat{\psi}(x,y)e^{iaz+\sigma t}, \tag{25a}$$

$$u_1 = \hat{u}(x,y)e^{iaz+\sigma t}, \tag{25b}$$

$$T_1 = \hat{T}(x,y)e^{iaz+\sigma t}, \tag{25c}$$

where a is real and represents the spanwise periodic wave number of the disturbances and σ is the growth factor. It is difficult to prove that σ is real, i.e. that the onset is stationary. However, we assume here, in analogy with many other convective instabilities, that σ is real. Substituting equations (25) into equations (22)–(24), the equations for neutral stability are

$$ia\hat{u} = \frac{\partial^2\hat{\psi}}{\partial x\partial y}, \tag{26}$$

$$\left(\frac{\partial^2\hat{\psi}}{\partial y^2} - a^2\hat{\psi}\right) = -\frac{iK\rho_\infty\beta g a\,\hat{T}}{\mu}, \tag{27}$$

$$\alpha\left[\frac{\partial^2\hat{T}}{\partial y^2} - a^2\hat{T}\right] = u_0\frac{\partial\hat{T}}{\partial x} + v_0\frac{\partial\hat{T}}{\partial y} + \hat{u}\frac{\partial T_0}{\partial x} - ia\hat{\psi}\frac{\partial T_0}{\partial y}. \tag{28}$$

To recast equations (26)–(28) in dimensionless form, the following dimensionless quantities will now be defined

$$k = \frac{ax}{(Ra_x)^{1/3}}, \quad F = \frac{\hat{\psi}}{i\alpha(Ra_x)^{1/3}}, \quad \Theta = \frac{\hat{T}}{Ax^m}, \tag{29}$$

where F and Θ are functions of η only. Equations (26)–(28) in terms of the dimensionless variables are

$$(D^2-k^2)F = -Ra_x^{1/3}k\Theta, \tag{30}$$

$$(D^2-k^2)\Theta = (Ra_x)^{1/3}\theta_0' kF - \frac{m+1}{3}f_0 D\Theta + mf_0'\Theta + \frac{(Ra_x)^{-1/3}}{3k}\left[\frac{(m-2)}{3}\eta\theta_0' + m\theta_0\right] \times [(m-2)\eta D^2F + (2m-1)DF], \tag{31}$$

with the boundary conditions given by

$$F(0) = \Theta(0) = 0, \tag{32}$$

$$F(\infty) = \Theta(\infty) = 0, \tag{33}$$

where $D \equiv d/d\eta$ is the differentiation of the disturbed quantities with respect to η. Note that in developing these equations we have eliminated $\hat{u}$ in favor of the stream function via equation (26). Substitution of equation (30) into equation (31) leads to

$$(D^2-k^2)^2F + \frac{m+1}{3}f_0 D(D^2-k^2)F - mf_0'(D^2-k^2)F + (Ra_x)^{2/3}\theta_0' k^2F + \frac{1}{3}\left[\left(\frac{m-2}{3}\right)\eta\theta_0' + m\theta_0\right] \times [(m-2)\eta D^2F + (2m-1)DF] = 0, \tag{34}$$

with its boundary conditions given by

$$F(0) = D^2F(0) = 0, \tag{35}$$

$$F(\infty) = D^2F(\infty) = 0. \tag{36}$$

For a given value of m and k, equation (34) with homogeneous boundary conditions (35) and (36) constitutes an eigenvalue problem where Ra_x can be regarded as the eigenvalue.

III. NUMERICAL SOLUTION OF THE EIGENVALUE PROBLEM

The eigenvalue problem can best be solved numerically by integrating equation (34) inward from $\eta \to \infty$ (the edge of the boundary layer of the base flow) to $\eta = 0$ (at the wall). To start the numerical integration at $\eta \to \infty$, asymptotic solutions for equation (34) will now be obtained. It is noted that equation (34) at large η is simplified to the constant coefficient type and its solutions are of the form

$$\begin{aligned} F_\infty^{(1)} &\sim e^{-k\eta}, \\ F_\infty^{(2)} &\sim e^{-[a_\infty + (a_\infty^2 + k^2)^{1/2}]\eta}, \\ F_\infty^{(3)} &\sim e^{k\eta}, \\ F_\infty^{(4)} &\sim e^{[a_\infty + (a_\infty^2 + k^2)^{1/2}]\eta}, \end{aligned} \tag{37}$$

where $a_\infty = f_0(\infty)(m+1)/6$ is a positive constant and η_∞ is some large value of η. Since the two exponential growing modes will not satisfy the boundary conditions at infinity, they must be discarded, and only the two decaying modes, $F^{(1)}$ and $F^{(2)}$ will be retained. Using $F_\infty^{(1)} = e^{-k\eta_\infty}$ and its derivatives as starting values at some large value of η (taken as $\eta_\infty = 8$ in the present study), equation (34) is integrated inward numerically by the fourth-order Runge–Kutta method to $\eta = 0$. The numerical solution thus obtained is denoted by $F^{(1)}(\eta)$. Similarly, a second numerical solution is obtained for $F^{(2)}(\eta)$ using $F_\infty^{(2)} = e^{-[a_\infty + (a_\infty^2 + k^2)^{1/2}]\eta_\infty}$ and its derivatives as its starting values at η_∞. It is worth noting that inside the boundary layer, equation (34) contains eigenfunctions which grow exponentially as $(Ra_x)^{1/3}$, which become singular for large Ra_x. Thus, in order to maintain the linear independence of the two numerical solutions at large Ra_x, Kaplan's filtering technique [14, 15] has been incorporated. The procedures involve the integration of $F^{(2)}(\eta)$ during the first path, and the filter applied at discrete steps of the second path for the integration of $F^{(1)}(\eta)$.

The complete solution to the linear equation (34) is a superposition of $F^{(1)}(\eta)$ and $F^{(2)}(\eta)$ which is given by

$$F(\eta) = F^{(1)}(\eta) + CF^{(2)}(\eta), \tag{38}$$

where the coefficient of $F^{(1)}(\eta)$ has been arbitrarily set equal to one. The constant C can be determined by imposing equation (38) on the boundary conditions at the wall, to give

$$F^{(1)}(0)+CF^{(2)}(0)=0, \tag{39}$$

$$D^2F^{(1)}(0)+CD^2F^{(2)}(0)=0, \tag{40}$$

where the values of $F^{(1)}(0)$, $F^{(2)}(0)$, $D^2F^{(1)}(0)$ and $D^2F^{(2)}(0)$ are already obtained from the numerical integration. Equations (39) and (40), in general, will not be compatible unless Ra_x is the eigenvalue. For a systematic iteration of Ra_x, we will first solve for C from equation (39) and substitute into equation (40) to give

$$D^2F^{(1)}(0)-\frac{F^{(1)}(0)}{F^{(2)}(0)}D^2F^{(2)}(0)=0, \tag{41}$$

which will not be satisfied unless Ra_x is the eigenvalue. If we denote the residue as

$$\Delta(Ra_x)=D^2F^{(1)}(0)-\frac{F^{(1)}(0)}{F^{(2)}(0)}D^2F^{(2)}(0), \tag{42}$$

then, a systematic iteration of Ra_x can be made by the Newton–Raphson iterative method until the condition $\Delta(Ra_x)=0$ is satisfied to within acceptable accuracy.

IV. RESULTS AND DISCUSSION

Consideration is first given to the neutral stability curves for selected values of m as shown in Fig. 2, where the eigenvalue Ra_x is plotted against dimensionless wave number k. The values of the critical Rayleigh number (Ra_x^*) and its associated wave number (k^*) are presented in Fig. 3 and Table 1, where it is shown that the values of Ra_x^* and k^* increase as the value of m is increased. It follows that $m=0$ represents the most unstable situation which is intuitively obvious since m

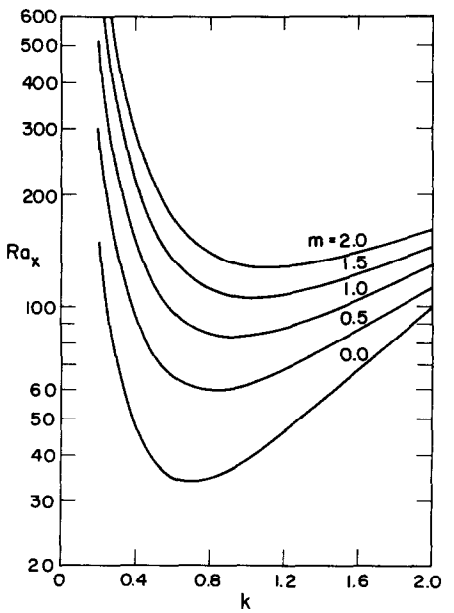

FIG. 2. Rayleigh numbers as a function of spanwise wave number at neutral stability.

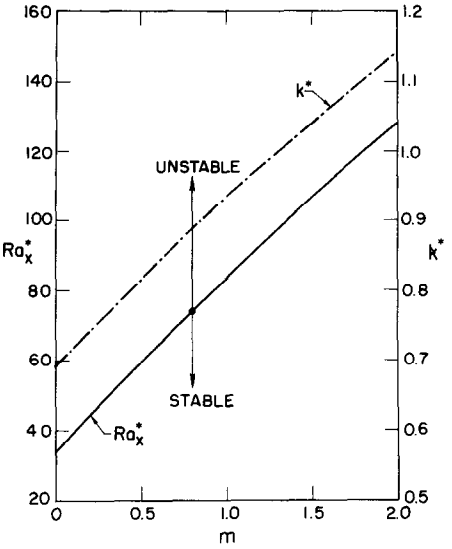

FIG. 3. Critical Rayleigh numbers and associated wave numbers as a function of m.

$=0$ corresponds to a step increase in wall temperature and thus is more susceptible to instability than other values of m which have a weaker rate of development in space of the ultimately unstable base state. A separate computation omitting the term $u_0(\partial T_1/\partial x)$ in equation (24) was also carried out. It was found that the critical Rayleigh numbers thus obtained were lower than those reported in Table 1, with the wave numbers essentially unchanged. Thus, the term $u_0(\partial T_1/\partial x)$ has a stabilizing effect on the flow field as is expected.

Table 1. Critical Rayleigh numbers and the associated wave numbers

m	Ra_x^*	k^*
0.0	33.47	0.692
0.5	59.78	0.815
1.0	83.46	0.934
1.5	106.23	1.041
2.0	128.63	1.141

Attention is next directed to the disturbances at the onset of instability. It can be shown that the dimensionless disturbances at the onset of instability are given by

$$\begin{aligned}
W &\equiv \frac{xw_1}{\alpha}=(Ra_x)^{2/3}DF\,e^{i(az+\pi/2)},\\
V &\equiv \frac{xv_1}{\alpha}=(Ra_x)^{2/3}kF\,e^{iaz},\\
U &\equiv \frac{xu_1}{\alpha}=(Ra_x)^{1/3}\left[\left(\frac{m-2}{3}\right)\frac{\eta}{k}D^2F\right.\\
&\left.+\frac{(2m-1)}{3k}DF\right]e^{iaz}\\
P &\equiv \frac{kp_1}{\mu\alpha}=\frac{(Ra_x)^{1/3}}{k}DF\,e^{i(az+\pi)},\\
\Psi &\equiv \frac{\psi_1}{\alpha}=(Ra_x)^{1/3}F\,e^{i(az+\pi/2)},\\
\theta &\equiv \frac{T_1}{Ax^m}=\Theta\,e^{iaz}
\end{aligned} \tag{43}$$

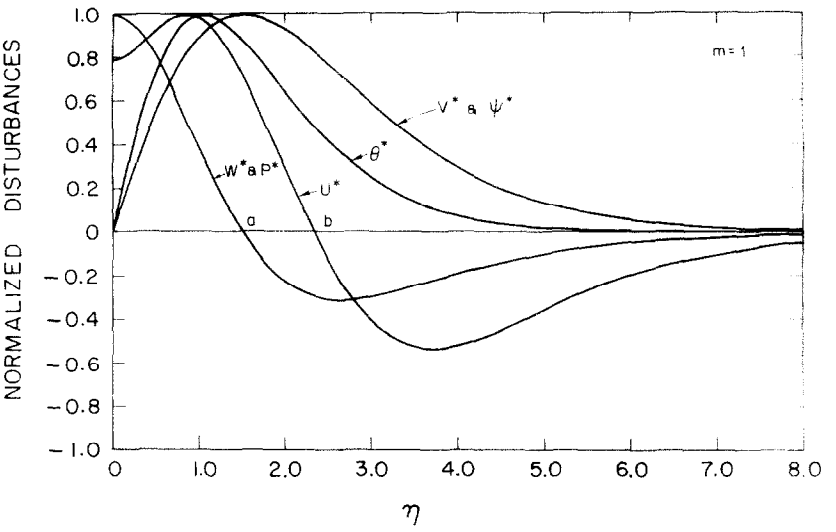

FIG. 4. The eigenfunctions for $m = 1$.

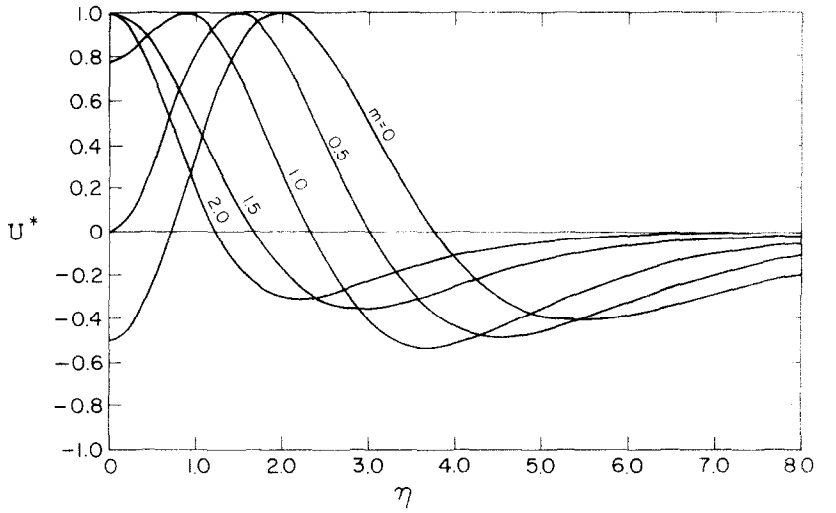

FIG. 5. The eigenfunction U^* for different values of m.

which show that U and P are of the same order, both of which are smaller than V and W. To plot the disturbed quantities vs η, it is convenient to normalize equation (43) with respect to their maximum values. It follows that normalized amplitudes W^*, V^*, U^*, P^*, Ψ^* and θ^* are given by

$$W^* = P^* = \frac{DF}{|DF|_{\max}},$$

$$V^* = \Psi^* = \frac{F}{|F|_{\max}}, \tag{44}$$

$$U^* = \frac{(m-2)\eta D^2F + (2m-1)DF}{|(m-2)\eta D^2F + (2m-1)DF|_{\max}},$$

and

$$\theta^* = \Theta/\Theta_{\max}.$$

Since the amplitudes W^*, V^*, P^*, Ψ^* and θ^* vs η have similar shapes for different values of m, only the representative profiles for $m = 1$ are plotted in Fig. 4. However, the amplitude U^* as a function of η changes drastically with m and are therefore plotted separately in Fig. 5. It is noted from Figs. 4 and 5 that while the values of V^* and Ψ^* are always positive, the values of W^* (or P^*) and U^* changes from positive to negative at $\eta = a$ and $\eta = b$ respectively. The change of signs of W^* and U^* simply indicate a change in the phase angle of π. Furthermore, it is noted in the figures that all the disturbances at the onset of instability are confined within the boundary layer of the basic flow which is consistent with the assumption of the bottling effect discussed earlier. The location of η for which $\Psi^*_{\max}$ and $\theta^*_{\max}$ occur are also of some interest. It is shown that the value of η at which $\theta^*_{\max}$ occurs is smaller than that of $\Psi^*_{\max}$.

It will also be of interest to examine the phase angles of disturbances (in the spanwise direction) relative to Ψ. Equations (43) show that θ and V are always ahead of Ψ by a phase angle of $\pi/2$. The phase angles of W, P and U with respect to Ψ however depends on the value of η. Near the wall where $\eta < a$, W is in phase with Ψ; P is behind Ψ by a phase angle of $\pi/2$; and U is

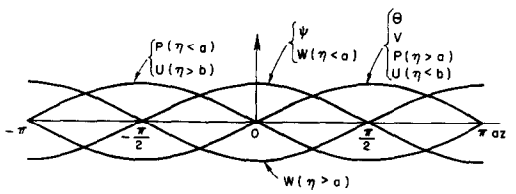

FIG. 6. Phase angles between disturbances for $m = 1$.

ahead of ψ by a phase angle of $\pi/2$. Near the edge of the boundary layer where $\eta > b$, W, P and U change their phase angle by π. The variations of disturbances along spanwise direction at a constant y at the onset of instability are sketched in Fig. 6. The corresponding streamlines and isotherms for the secondary flow at the onset of instability are indicated as solid and dashed lines in Fig. 7.

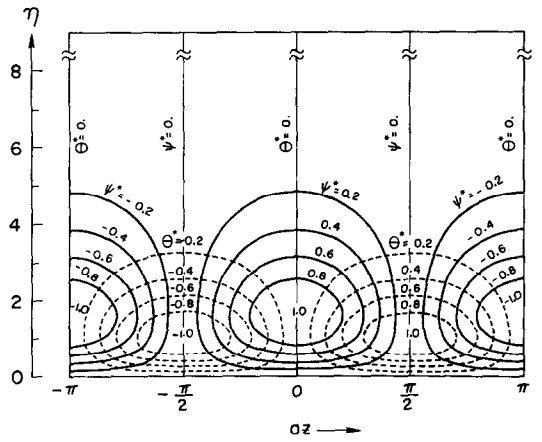

FIG. 7. Secondary flow streamlines and isotherms for $m = 1$.

To summarize, the analysis given here predicts the distance from the leading edge at which the buoyancy layer first becomes unstable. The form of the instability is a roll vortex with a weak down-stream dependence. The wave length of the roll scales with the local depth of the thermal layer.

Acknowledgements—P. Cheng wishes to thank the Institute for Energy Studies and the Petroleum Engineering Department of Stanford University, and the National Science Foundation (through Grant ENG77-27527) for partial support. G. Homsy acknowledges the support of the NSF through Grant ENG73-93955.

REFERENCES

1. K. Chandra, Instability of fluids heated from below, *Proc. R. Soc.* **A164**, 231–242 (1938).
2. M. Akiyama, G. J. Hwang and K. C. Cheng, Experiments on the onset of longitudinal vortices in laminar forced convection between horizontal plates, *J. Heat Transfer* **93**, 335–341 (1971).
3. E. M. Sparrow and R. B. Husar, Longitudinal vortices in natural convection flow on inclined plates, *J. Fluid Mech.* **37**, 251–255 (1969).
4. J. R. Lloyd and E. M. Sparrow, On the instability of natural convection flow on inclined plates, *J. Fluid Mech.* **42**, 465–470 (1970).
5. G. J. Hwang and K. C. Cheng, Convective instability of laminar natural convection flow on inclined isothermal plates, *Can. J. Chem. Engng* **51**, 659–666 (1973).
6. S. E. Haaland and E. M. Sparrow, Vortex instability of natural convection flow on inclined surfaces, *Int. J. Heat Mass Transfer* **16**, 2355–2367 (1973).
7. P. A. Iyer and R. E. Kelly, The stability of the laminar free convection flow induced by a heated inclined plate, *Int. J. Heat Mass Transfer* **17**, 517–525 (1974).
8. R. A. Kahawita and R. N. Meroney, The vortex mode of instability in natural convection flow along inclined plates, *Int. J. Heat Mass Transfer* **17**, 541–548 (1974).
9. W. Nakayama, G. J. Hwang and K. C. Cheng, Thermal instability in plane Poiseuille flow, *J. Heat Transfer* **92**, 61–68 (1970).
10. G. J. Hwang and K. C. Cheng, Convective instability in the thermal entrance region of a horizontal parallel-plate channel heated from below, *J. Heat Transfer* **95**, 72–77 (1973).
11. R. S. Wu and K. C. Cheng, Thermal instability of Blasius flow along horizontal plates, *Int. J. Heat Mass Transfer* **19**, 907–913 (1976).
12. S. A. Bories and M. A. Combarnous, Natural convection in a sloping porous layer, *J. Fluid Mech.* **57**, 63–79 (1973).
13. P. Cheng and I.-Dee Chang, Buoyancy-induced flows in a porous medium adjacent to impermeable horizontal surfaces, *Int. J. Heat Mass Transfer* **19**, 1267–1272 (1976).
14. R. Betchov and W. O. Criminale, *Stability of Parallel Flows*. Academic Press, New York (1967).
15. R. E. Kaplan, The stability of laminar incompressible boundary layers in the presence of compliant boundaries, M.I.T. Aero-Elastic and Structures Research Laboratory, ASRL-TR 116-1 (1964).

INSTABILITE DE L'ECOULEMENT DE CONVECTION NATURELLE SUR UNE SURFACE HORIZONTALE ET IMPERMEABLE DANS UN MILIEU POREUX

Résumé—Une analyse linéaire de stabilité est faite pour déterminer les conditions d'apparition de tourbillons longitudinaux dans la convection naturelle dans un milieu poreux adjacent à une surface chaude horizontale avec une température de paroi prescrite. L'état de base est supposée être l'écoulement de couche limite induite qui est caractérisé par un profil de température non linéaire. On prend en considération la composante transversale de la vitesse de l'écoulement de base ainsi que la dépendance des champs de vitesse et de température, pour établir les équations de perturbation tridimensionnelle de l'écoulement secondaire. Le problème résultant des valeurs propres est résolu numériquement et les amplitudes et les phases des perturbations sont données ainsi que les lignes de courant et les isothermes de l'écoulement secondaire à l'apparition de l'instabilité. On discute de l'effet de la distribution de la température pariétale sur le nombre de Rayleigh et sur le nombre d'onde associé.

INSTABILITÄT EINER FREIEN KONVEKTIONSSTRÖMUNG ÜBER EINER WAAGERECHTEN, UNDURCHLÄSSIGEN FLÄCHE IN EINEM PORÖSEN MEDIUM

Zusammenfassung—Es wurde eine lineare Stabilitätsanalyse durchgeführt, um die Bedingungen zu bestimmen, die kennzeichnend sind für den Beginn von Längswirbeln in einer freien Konvektionsströmung in einem porösen Medium, das an eine waagerechte, beheizte Fläche mit vorgegebener Wandtemperatur angrenzt. Als Grundzustand ist die stationäre, zweidimensionale, auftriebsinduzierte Grenzschichtströnung angenommen, die durch ein nichtlineares Temperaturfeld charakterisiert ist. Sowohl die Querkomponente der Geschwindigkeit der Grundströmung als auch die Abhängigkeit zwischen Grundströmung und Temperaturfeld in Strömungerichtung werden beim Ableiten der dreidimensionalen Strömungsgleichungen für die Sekundärströmung berücksichtigt. Das resultierende Eigenwert-Problem mit variablem Koeffizienten wird numerisch gelöst und sowohl die Amplituden und Phasenwinkel der Störungen als auch die Stromlinien und die Isothermen der Sekundärströmung bei Beginn der Instabilität werden ermittelt. Der Einfluß der Wandtemperaturverteilung auf die kritische Rayleigh-Zahl und die entsprechend zugeordnete Wellenzahl werden diskutiert.

НЕУСТОЙЧИВОСТЬ СВОБОДНОКОНВЕКТИВНОГО ТЕЧЕНИЯ НА ГОРИЗОНТАЛЬНОЙ НЕПРОНИЦАЕМОЙ ПОВЕРХНОСТИ В ПОРИСТОМ ТЕЛЕ

Аннотация — Проведен линейный анализ устойчивости свободноконвективного течения для определения условий возникновения продольных вихрей в пористой среде на горизонтальной нагретой поверхности с заданной температурой. Предполагается стационарное двухмерное свободноконвективное течение в пограничном слое в пористой среде с нелинейным профилем температур. При выводе трехмерных уравнений возмущения для вторичного течения учитываются поперечная компонента скорости основного потока, а также зависимость полей основного потока и температуры от расстояния вдоль потока. Даётся численное решение полученной задачи на собственные значения с переменными коэффициентами. Приведены амплитуды и фазовые углы возмущений, а также линии тока и изотермы вторичного течения при возникновении неустойчивости. Обсуждается влияние распределения температуры на стенке на критическое число Релея и соответствующее волновое число.